



## Experimental Investigation of Flooding and Drop Size in a Kuhni Extraction Column

A.R. Shirvani,<sup>a</sup> A. Ghaemi \*<sup>a</sup>, M. Torab-Mostaedi<sup>b</sup>

<sup>a</sup> Department of Chemical Engineering, Iran University of Science and Technology

<sup>b</sup> Nuclear Fuel Cycle Research School, Nuclear Science and Technology Research Institute

### PAPER INFO

#### Paper history:

Received 18 October 2015

Received in revised form 20 February 2016

Accepted 03 March 2016

#### Keywords:

Kuhni Column

Flood Point

Holdup

Sauter-Mean Drop Diameter

### A B S T R A C T

In this work, the hydrodynamic behavior of a Kuhni extraction column has been investigated experimentally. The experiments were carried out in the absence of mass transfer for two different standard chemical systems. In the experiments operating variables including agitation speed, flow rate of both liquid phases and interfacial tension have been studied. Sauter-mean drop diameter, flooding velocity and holdup at flooding have been measured in the Kuhni column. The results showed that Sauter-mean diameter are strongly affected by agitation speed and interfacial tension whereas the effects of continuous phase and dispersed phase flow rates are negligible. Two rigorous empirical correlations are proposed for predicting flooding velocities and Sauter-mean drop diameter with mean deviation of 5.7% and 7.2%, respectively. The mean drop size correlation is a function of column geometry, operating conditions and physical properties of liquid systems. Good agreement between predictions and experiments is found for all operating conditions investigated.

doi: 10.5829/idosi.ije.2016.29.03c.02

## 1. INTRODUCTION

The liquid-liquid extraction as one of the important processes of mass and energy exchange with the extensive application in the petroleum and petrochemical industries, nuclear industries, pharmaceutical industries, metallurgy [1-4]. The operations consist in separation of one or several components (solute) from a liquid phase mixture by addition of another non-miscible or partially miscible liquid phase, in which the solute is preferentially dissolved. This operation process is often operated in counter-current contactors [5]. Two immiscible liquid phases flow counter-currently, one being dispersed into the other. Each extraction equipment attempts to produce larger interfacial area often by applying mechanical agitation to better disperse the phase [6]. Kühni column is representatives of this type of equipment. In this column, worn blades on a central

shaft used and steps separated by a leaky static plate. Blades create a vortex flow pattern which is somewhat similar to RDC column [7]. Also, perforated plates used between stages make it possible to creating axial flow in column but completely separated steps than RDC and MIXCO columns. This topic caused reduction reverse flow especially for the dispersed phase, but collects and unlocks the column for cleaning and maintenance makes it more difficult. Kühni columns in the range of sizes laboratory scale by 60 mm diameter to industrial scale by 2 m diameter and with similar applications to RDC are existence [8].

For the design, optimization and exploitation of extraction column require both mass transfer and hydrodynamic parameters, such as holdup, flooding velocities and drop size distribution. Holdup, flooding velocities and drop size, are key parameters in order to determine the column capacity and the column diameter [9]. Knowledge of drop size and distribution are necessary parameters for measuring mass transfer coefficients [10]. It influences the dispersed phase holdup and residence time and the maximum capacity of the column [9, 11]. Thus, for the purpose of establishing

\*Corresponding Author's Email: [aghaemi@iust.ac.ir](mailto:aghaemi@iust.ac.ir) (A. Ghaemi)

suitable design procedures for Kühni columns, there is a need for valid correlations which estimate Sauter-mean drop diameter and flooding conditions.

In this work, the hydrodynamic behavior of a Kühni column was investigated by measuring the Sauter-mean drop diameter and flood point characteristics using two different liquid systems. The effects of operating variables on mean drop size and flood point are examined. In addition, experiential correlations for mean drop size and flooding velocities as a function of operating conditions, physical properties of the liquid systems and column geometry were proposed.

## 2. EXPERIMENTS

**2.1. Description of Experimental Setup** A pilot scale Kühni extraction column with ten stages that made of 2 mm perforated stainless steel sheet was used in the experiments. The active part of the column consisted of a 0.75 m long glass tube with 0.117 m internal diameter. Two settlers with 0.1775 m diameter were employed at both ends of the column to separate the two liquid phases. There are two pumps, one for the dispersed phase and one for the continuous phase. The interface level was controlled automatically by an optical sensor. A solenoid valve was provided at the outlet stream of the heavy phase. This valve received electronic signals from the sensor. When the interface location was going to change, the optical sensor sent a signal to the solenoid valve and the aqueous phase was allowed to leave the column by opening the diaphragm of the solenoid valve. The organic phase was allowed to leave the column via overflow. Other geometrical characteristics of the column are presented in Table 1. The schematic diagram of Kühni extraction column is shown in Figure 1.

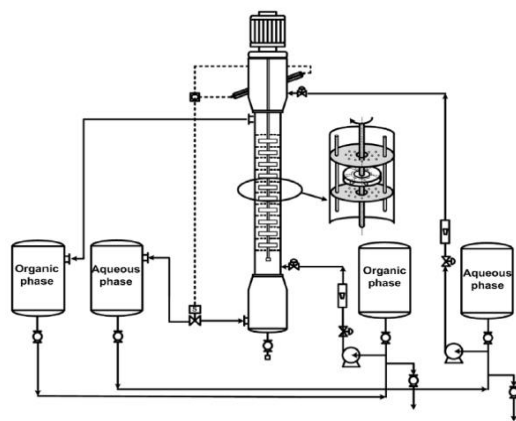


Figure 1. A schematic diagram of the Kühni column

TABLE 1. Technical parameters of Kühni extraction column.

Parameter	Value	Parameter	Value
Column diameter (m)	0.117	Settler diameter(m)	0.1775
Tray number	10	Active volume of the column(m <sup>3</sup> )	0.0075
Number of holes	27	Impeller diameter (m)	0.05
Tray perforation diameter (m)	0.0075	Plate thickness(m)	0.002
Column height(m)	0.7	Compartment height(m)	0.055

TABLE 2. Physical properties of liquid systems

Physical property	Toluene–water	n-Butyl acetate–water
$\rho_c$ (kg/m <sup>3</sup> )	998.2	997.6
$\rho_d$ (kg/m <sup>3</sup> )	865.2	880.9
$\mu_c$ (m Pas)	0.963	1.027
$\mu_d$ (m Pas)	0.584	0.734
$\sigma$ (mNm <sup>-1</sup> )	36.0	14.1

**2. 2. Liquid-Liquid Systems** Two liquid-liquid system to cover a wide range of interfacial tension values were chosen according to the recommendations of the European Federation of Chemical Engineering [12]. The liquid-liquid systems that studied were toluene–water (high interfacial tension), n-butyl acetate–water (medium interfacial tension). The technical grade, solvents at least 99.5 wt % purity were used as the dispersed phase. All experiments were carried out at the  $20 \pm 2^\circ\text{C}$ . The physical properties of the liquid-liquid systems used in the experiments are shown in Table 2.

## 3. FLOOD POINT AND HOLDUP MEASUREMENTS

In the design of an extraction column, the hydrodynamic parameters including holdup and flooding velocities are key parameters in order to determine the column capacity and the column diameter required. The Number of correlations to predict flooding velocities in different columns is presented in Table 3. It shows that flooding velocity correlations are presented as a function of operating conditions, physical properties of the liquid systems and column geometry are proposed [13-15].

In present work, every liquid phase was first saturated with the other as this is specially necessary when the organic phase and aqueous phase have significant reciprocal solubility, and the impeller speed were equaled to the desired values.

**TABLE 3.** Number of correlations to predict flooding in different columns

Extraction column type	Correlation	Reference
Pulsed packed	$\frac{(V_c^{0.5} + V_d^{0.5})\rho_c}{a\mu_c} = 0.5303e^{0.05} \left(\frac{\Delta\rho}{\rho_c}\right)^{-0.256} \left(\frac{\mu_d^2 d_T g}{\gamma^2}\right)^{-0.051} \left(\frac{a^3 \mu_c^2}{g\Delta\rho}\right)^{-0.252} \left(\frac{\gamma\rho_c}{\mu_c^2 a}\right)^{0.283} \left(\frac{Af\rho_c}{a\mu_c}\right)^{-0.11}$	[14]
Pulsed packed	$\frac{(V_c^{0.5} + V_d^{0.5})\rho_c}{a\mu_c} = 0.5303e^{0.05} \left(\frac{\Delta\rho}{\rho_c}\right)^{-0.256} \left(\frac{\mu_d^2 d_T g}{\gamma^2}\right)^{-0.051} \left(\frac{a^3 \mu_c^2}{g\Delta\rho}\right)^{-0.252} \left(\frac{\gamma\rho_c}{\mu_c^2 a}\right)^{0.283} \left(\frac{Af\rho_c}{a\mu_c}\right)^{-0.11}$	[14]
Pulsed disc and doughnut	$\frac{(V_{cf} + V_{df})\mu_c}{\sigma} = 10.80*10^3 \left(\frac{\Delta\rho}{\rho_c}\right)^{-0.484} \left(\frac{d_a \rho_c \sigma}{\mu_c^2}\right)^{-1.407} \left(\frac{\Psi \mu_c^5}{\rho_c \Psi^4}\right)^{-0.17} \left(\frac{d_c}{d_a}\right)^{13.07} (1+R)^{-0.283}$	[15]
Pulsed disc and doughnut	$V_{df} = 2.11*10^3 \left(\frac{Af^4 \rho_c}{g\sigma}\right)^{-0.124} \left(\frac{\Delta\rho}{\rho_c}\right)^{0.336} (1+R)^{0.511}$	[13]
Hanson Mixer-Settler	$\frac{V_{df} \rho_c^{0.25}}{g^{0.25} \sigma^{0.25}} = 1.48 \left(\frac{g}{N^2 D}\right)^{0.23} \left(\frac{\Delta\rho}{\rho_c}\right)^{-0.40} \left(\frac{\eta_d}{\eta_c}\right)^{0.20} (1+L)^{0.32}$	[13]

The continuous phase was first set at the desired flow rate. The dispersed phase was then slowly entered, and its flow rate was slowly increased until the flooding point, as revealed by the first appearance of a thin layer of the dispersed phase under the each step or by the rejection of the dispersed phase in the form of a dense layer of small droplets, was reached. The reliability of flooding rates was within  $\pm 5\%$ . When the flooding happened, input and output of the column were shut down suddenly and allowed to the dispersed phase to go to the interface at the top of the column.

#### 4. DROPLET SIZE MEASUREMENTS

According to the importance of droplet size, many researchers studied the effect of column operating variables on drop size and developed correlations for predicting the mean drop size [16-24]. Drop size affects almost all the parameters that influence hydrodynamics and mass transfer in an extraction column [9]. The drop size developed for different extractors are presented in Table 4. It shows that drop size depend on column geometry, phases properties and flow rates and agitation speed. In this work, to measure the drop diameter a photographic technique was used. By taking a digital photo of the column by a Nikon D3100 digital camera and comparing the drop dimensions with the known size of column as a reference droplet size were obtained. For this comparison two characteristic lengths of the internals were used, being the tray thickness and spacing,  $h_c$ . The recorded photos were analyzed with image processing software to determine the size of the drops. At least 300 drops were analyzed for each

experimental condition. For elliptical drops, both the minor and major axes,  $d_1$  and  $d_2$ , were measured and the equivalent diameter,  $d_e$ , calculated from the following equation:

$$d_e = \left(d_1^2 d_2\right)^{\frac{1}{3}} \quad (1)$$

After the determination of the drop sizes, the Sauter-mean drop diameter,  $d_{32}$ , was calculated at experimental conditions used as follows:

$$d_{32} = \frac{\sum_{i=1}^n n_i d_i^3}{\sum_{i=1}^n n_i d_i^2} \quad (2)$$

where,  $n_i$  is the number of droplets of mean diameter  $n_i$  within a narrow size range  $i$ .

#### 5. NUMERICAL METHODS

Numerical solutions including Genetic Algorithms (GA) and Particle Swarm Optimization (PSO) were used to obtain optimum values of flooding velocities and drop size correlations parameters. GA is a search method to find an approximate solution optimization problem using the concepts of biology such as inheritance and mutations [25-29]. In this algorithm based on Darwin's theory of evolution, the problem variables by using appropriate binary strings are coded. Then, by simulation of struggle for survival rules, regularly more appropriate disciplines (that in fact, represents the improved solutions) are obtained. Like other optimization techniques, GA is an optimization method

based on probabilities, namely to ensure obtaining the general optimal solution, in any given optimization problem this algorithm is run several times and compare the results [27-29]. Also, the probability of finding global optimum solution by GA is very high. To solve the minimization problems before applying GA should be convert the problem to a maximization problem [25]. The most common way is to define a fitness function, the contrast is a linear combination of the cost function. For example, if the goal of the optimization is to find the minimum of the function,  $f(x)$  and this function will return the value of all slopes greater than -1 then it can be used to define the fitness function.

$$F(x) = \frac{1}{1 + f(x)} \tag{3}$$

PSO is a population based stochastic optimization technique, inspired by social behavior of bird flocking or fish schooling [25, 26]. PSO shares many similarities

with evolutionary computation techniques such as GA. The system is initialized with a population of random solutions and searches for optima by updating generations. However, unlike GA, PSO has no evolution operators such as crossover and mutation. In PSO, the potential solutions, called particles, fly through the problem space by following the current optimum particles [25].

Each particle keeps track of its coordinates in the problem space which are associated with the best solution (fitness) it has achieved so far (The fitness value is also stored). This value is called pbest. Another "best" value that is tracked by the particle swarm optimizer is the best value, obtained so far by any particle in the neighbors of the particle. This location is called lbest. When a particle takes all the population as its topological neighbors, the best value is a global best and is called gbest.

**TABLE 4.** Number of correlations to predict droplet size in different columns

Extraction column type	Correlation	Reference
Pulsed packed	$\frac{1}{d_{32}} - 0.72 \left( \frac{\Delta\rho g}{\sigma} \right)^{0.5} = 6700 \left( \frac{1-\Phi}{\Phi} \right) \left( \frac{fA\rho_c}{\eta_c a_p} \right) \left( \frac{\eta_c^2 a_p}{\sigma\rho_c} \right)^{0.5} \left( \frac{\sigma a_p^2}{\Delta\rho g} \right)^{0.23}$	[16]
Pulsed perforated-plate	$\frac{d_{32}}{\sqrt{\frac{\sigma}{\Delta\rho g}}} = 1.35\alpha^{0.40} \left( \frac{1}{\sqrt{\frac{\sigma_w}{\sigma_w g}}} \right)^{0.18} \left( \frac{\mu_d g^{0.25}}{\rho_w^{0.25} \sigma_w^{0.75}} \right)^{0.14} \left( \frac{\sigma}{\sigma_w} \right)^{0.06} \times \left[ 0.23 + \exp \left( -29.66 \frac{Af^2}{g\alpha} \right) \right]$	[17]
Stirred Tank	$d_{32} = C_2 \varepsilon^{-0.4} \left( \frac{\gamma}{\rho_c} \right)^{0.6} [1 + C_3 \left( \frac{\rho_c}{\rho_d} \right)^{1/2} \frac{\mu_d \varepsilon^{1/3} d_{32}^{1/3}}{\gamma}]^{3/5}$	[18]
Wirz	$d_{32} = (1 + 1.78\phi) \left[ \frac{1}{[0.98 \left( \frac{\gamma}{\Delta\rho g} \right)^{0.5}]^2} + \frac{1}{[0.27 \varepsilon^{-0.4} \left( \frac{\gamma}{\rho_c} \right)^{0.6}]^2} \right]^{1/2}$	[19]
Single drop	$\frac{d_{32}}{Dl} = 0.081(1 + 4.47\phi) w e_l^{-0.06}$ , $\frac{d_{32}}{Dl} = 0.053(1 + 4.42V_i) w^{0.6} e_l^{-0.06}$	[13]
Pulsed Packed	$d_{32} = C_1 \left( \frac{\sigma}{\Delta\rho g} \right)^{0.5} \left( \frac{\sigma}{Af\eta_c} \right)^{C_2} \left( 1 + \frac{V_d}{V_c} \right)^{C_3}$	[30]
Pulsed packed	$d_{32} = -0.33 + 4.375 \exp \left( \frac{-Af}{0.042} \right)$	[14]
Pulsed disc and doughnut	$\frac{d_{32}}{\sqrt{\frac{\sigma}{\Delta\rho g}}} = 33.53 * 10^{-3} \left( \frac{Af^4 \rho_c}{g\sigma} \right)^{-0.283} \left( \frac{d_a \rho_c \sigma}{\mu_c^2} \right)^{0.29} \left( \frac{\rho_c \sigma^4}{\Psi \mu_c} \right)^{-0.013} \left( \frac{\Delta\rho}{\rho_c} \right)^{2.86} \left( \frac{\mu_d}{\mu_c} \right)^{0.085} \left( \frac{h_c}{d_a} \right)^{-0.734} (1+R)^{0.34}$	[15]
Hanson Mixer-Settler	$d_{32} = 0.23(1 + 2.24\Phi) We^{-0.6} \left( \frac{\eta_d}{\eta_c} \right)^{-1.14}$ , $d_{32} = 0.197(1 + 3.04\Phi) We^{-0.6} \left( \frac{\eta_d}{\eta_c} \right)^{-1.27}$	[13]
Pulsed packed	$d_{32} = 8.26 * 10^{-5} \left( \frac{(af)^4 \rho_c}{\sigma g} \right)^{-0.2304} \left( \frac{\mu_c^4 g}{\Delta\rho \sigma^3} \right)^{-0.0514} \left( 1 + \frac{Q_c}{Q_d} \right)^{0.0321}$	[30]
Pulsed packed	$d_{32} = 7.1 * 10^{-5} \left( \frac{(af)^4 \rho_c}{\sigma g} \right)^{-0.239} \left( \frac{\mu_c^4 g}{\Delta\rho \sigma^3} \right)^{-0.0473} \left( \frac{h}{H_0} \right)^{-0.1645}$	[30]

The PSO concept consists of, at each time step, changing the velocity of each particle toward its pbest and lbest locations [25]. Acceleration is weighted by a random term, with separate random numbers being generated for acceleration toward pbest and lbest locations. The calculation flowchart is shown in Figure 2.

## 6. RESULTS AND DISCUSSION

**6.1. Sauter-Mean Drop Diameter** Agitation speed and phase flow rates are the most important parameters that have effect on droplet size. The effect of agitation speed on Sauter-mean drop diameter is shown in Figure 3. It shows that smaller drops are observed at higher rotor speeds, that is a result of increased droplet break-

up. Although the decrease in Sauter-mean diameter at a higher rotor speeds is smooth. Coalescence of droplets at high rotor speeds is increased by increasing the probability of droplet collision. So, at the high rotor speeds, the increased rate of coalescence dominance the increased sentiment for droplet breakage and the drop size apparently stabilized. Figure 3 also shows that an increase in the interfacial tension results in an increase in drop diameter. The effect of dispersed phase velocity on the mean drop size is shown in Figures 4 and 5. As shown in Figure 4, increasing the dispersed phase flow rate tends to increase the mean drop size. Increasing in dispersed phase velocity cause to a larger drop formation diameter and a higher coalescence frequency.

Figures 6 and 7 also show that the effect of dispersed phase velocity grows in importance as the interfacial tension of the system increases.

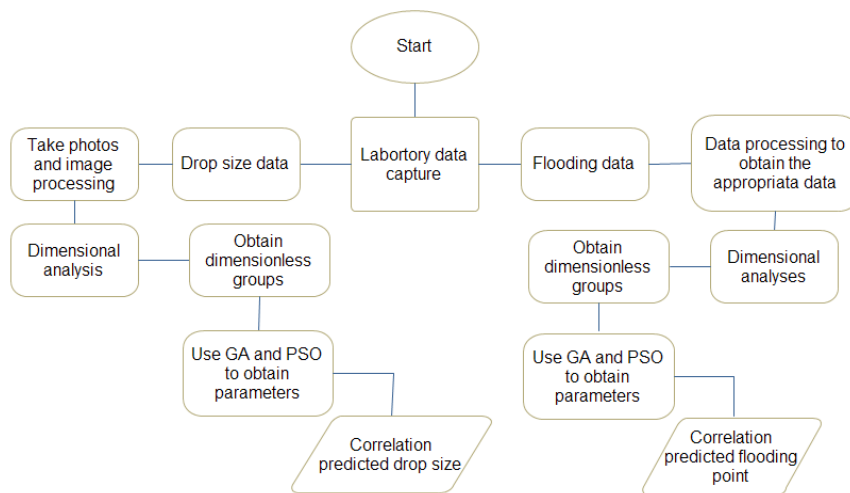


Figure 2. Calculation flowchart of drop size and flooding point

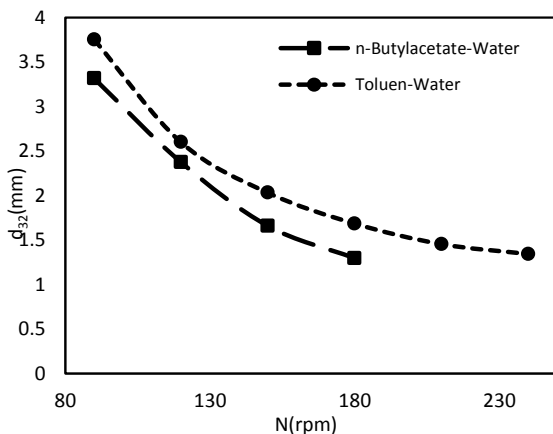


Figure 3. Effect of rotor speed on mean drop size  $Q_d=Q_c=24$  lit/hr

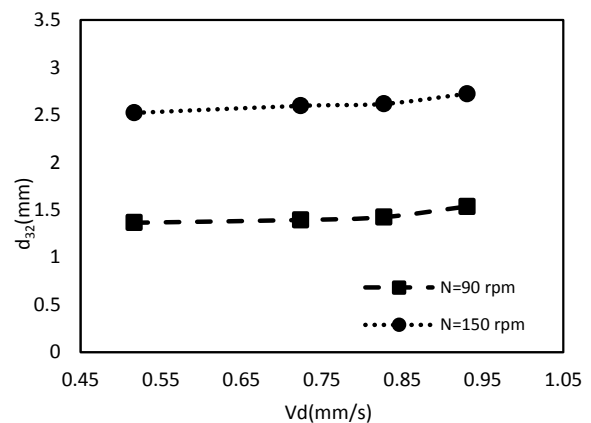
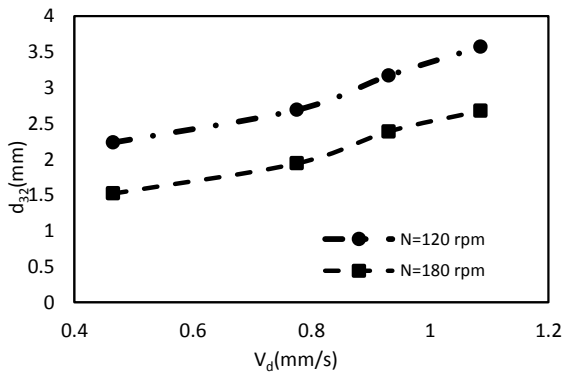


Figure 4. Effect of dispersed phase velocity on mean drop size  $Q_c=24$  lit/hr, n-butyl acetate-water



**Figure 5.** Effect of dispersed phase velocity on mean drop size  $Q_C = 24 \text{ lit/hr}$ , Toluene-water

**6.2. Prediction of Sauter-mean Drop Diameter** One of the main objectives of this study is to propose a new correlation for prediction of mean drop size. Since a correlation for the mean drop size,  $d_{32}$ , in Kuhni column is not available, Kumar and Hartland [11] Used Equation (4) to predict the Sauter-mean drop diameter. This correlation is proposed for predicting mean drop size in Kuhni column. The parameters of this correlation for Kuhni column are shown in Table 5. Equation (4) reproduces the experimental results with an average relative deviation (ARE) of 26.8%.

$$d_{32} = C_{\psi} e^n \left[ \frac{1}{[C_{\Omega} (\frac{\gamma}{\Delta\rho g})^{0.5}]^2} + \frac{1}{[C_{\Pi} \varepsilon^{-0.4} (\frac{\gamma}{\rho_c})^{0.6}]^2} \right]^{1/2} \tag{4}$$

To obtain the sound correlation for predicting the mean drop size, dimensional analysis with considering an influencing parameters such as the geometry of column, operating conditions and physical properties of liquid systems was used. The following equation for the mean drop size was obtained using the Buckingham theorem. In order to consider the column geometry effect on Sauter-mean drop diameter and also to increase the total number of data points, the experimental results are taken from Oliveira et al. [31] for water-Exxsol D-80 system.

$$d_{32} = n_1 \left( \frac{V_c}{V_d} \right)^{n_2} \left( \frac{\mu_d N}{V_d^2 \Delta\rho} \right)^{n_3} \left( \frac{V_d \Delta\rho D_{cu}}{\mu_d} \right)^{n_4} \left( \frac{V_d \Delta\rho D_{im}}{\mu_d} \right)^{n_5} \left( \frac{\mu_c}{\mu_d} \right)^{n_6} \left( \frac{\rho_c}{\Delta\rho} \right)^{n_7} \left( \frac{\sigma}{\mu_d V_d} \right)^{n_8} \left( \frac{\mu_d g \varepsilon}{V_d^3 \Delta\rho} \right)^{n_9} \left( \frac{\mu_d}{\Delta\rho V_d} \right) \tag{5}$$

**TABLE 6.** optimum parameters values of Equation (5)

Num.Method	$n_1$	$n_2$	$n_3$	$n_4$	$n_5$	$n_6$	$n_7$	$n_8$	$n_9$	ARD%
GA	2.062	0.234	-1.097	1.579	-0.762	2.257	-2.022	-0.371	0.591	5.70
PSO	2.062	0.234	-1.094	1.579	-0.759	2.257	-2.022	-0.372	0.591	5.70

To fit the experimental data and to obtain the parameters and minimize the relative absolute error, the following objective function was minimized.

$$ARD\% = 100 \times \frac{\left| (d_{32}^{exp} - d_{32}^{cal}) \right|}{d_{32}^{exp}} \tag{6}$$

Numerical solutions including GA and PSO were used to obtain optimum values of Equation (5) parameters. The results of this optimization were presented in Table 6.

**6.3. Flood Point** The results of flooding and holdup at different rotor speeds are shown in Figures 6 to 7. As shown in these figures, with increase in continuous phase velocity the allowable dispersed phase velocity is decreases. The slip velocity between the phases is reduced by increasing the continuous phase velocity. Therefore, the dispersed phase holdup increases with increase in continuous phase velocity and consequently the column becomes unstable at lower dispersed phase velocities. The drop size is decrease with increasing rotor speed, which results in an increasing hold-up such that the critical hold-up is reached at a lower total throughput. From Figures 9 and 10, it can be concluded that by increasing rotor speeds, the maximum throughput of the column decreases.

**6.4. Predictive Correlation for Flooding Velocities** In this work an empirical correlation to represent the flooding velocities in Kuhni columns was derived. This correlation is mainly based on the operating variables and the system physical properties. This correlation could be used to predict maximum throughput for existing Kuhni columns.

$$V_{gf} = n_1 \left( \frac{\mu_d}{\mu_c} \right)^{n_2} \left( \frac{\rho_c}{\Delta\rho} \right)^{n_3} \left( \frac{\sigma}{V_c \mu_c} \right)^{n_4} \left( \frac{\mu_c g}{\Delta\rho V_c^3} \right)^{n_5} \left( \frac{\mu_c N}{\Delta\rho V_c^2} \right)^{n_6} V_c \tag{7}$$

**TABLE 5.** Parameters of Equation (4) For Kuhni column[8]

Column type	No. of data	$C_{\psi}$ c→d	$C_{\psi}$ d→c	$C_{\Omega}$	$C_{\Pi}$	n	ARD%
Kuhni	704	1	3.05	2.49	0.52	0.57	26.8

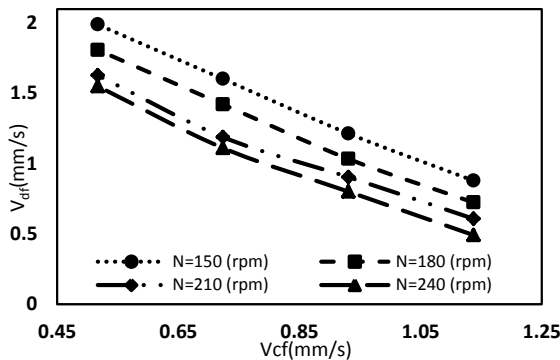


Figure 6. Experimental variation in  $V_{df}$  with  $V_{cf}$  (n-butyl acetate –Water).

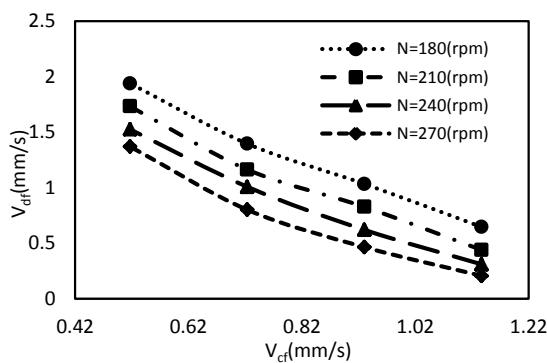


Figure 7. Experimental variation in  $V_{df}$  with  $V_{cf}$  (Toluene – Water).

TABLE 7. Optimum parameters values of Equation 7

Method	$n_1$	$n_2$	$n_3$	$n_4$	$n_5$	$n_6$	ARD%
GA	2.89	-9.93	-3.60	-1.97	2.27	-1.18	11.56
PSO	2.82	-9.97	-3.59	-1.98	2.28	-1.18	11.54

In order to reduce error and increase the accuracy, the numerical methods including GA and POS were used to obtain the optimum parameters of Equation (7). The methods were used to fit the experimental data and to obtain the parameters and minimize the relative absolute error. The results are presented in Table 7. The relative absolute error (ARD%) the following objective function was minimized.

$$ARD\% = 100 \times \frac{|(V_f^{Exp.} - V_f^{Cal.})|}{V_f^{Exp.}} \quad (8)$$

The comparison of the experimental data with those calculated by Equation (7) is shown in Figure 8. This figure shows that the experimental results are in good agreement with calculated values obtained by Equation (7). This correlation reproduces the experimental results with an average relative deviation of 7.2 %.

## 7. COMPARISON OF PREVIOUS MODELS WITH THE EXPERIMENTAL RESULTS

Various correlations for predicting flooding velocities are available in the literature. The relative absolute error, (ARD%) of the calculated values of flooding velocities obtained by applying the previous correlations to the experimental results are listed in Table 8. The results show that the previous models do not practically have accurate results. The results show that the presented correlation has good accuracy.

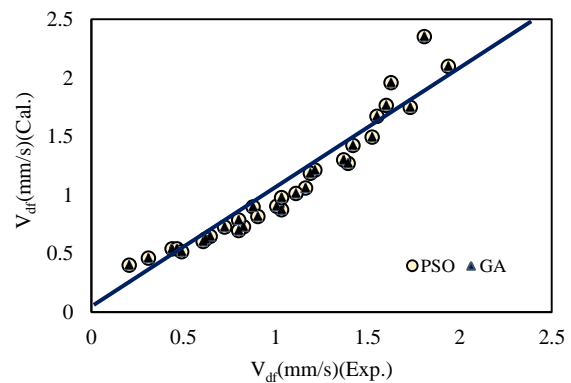


Figure 8. Comparison between experimental data and the predictions of Equation (7).

TABLE 8. ARD for different models of flooding velocities

Investigator	Column type	ARD(%)
Gholam Samani et al. [30]	pulsed packed	8.80
Gholam Samani et al. [30]	pulsed packed	7.80
Ousmane[22]	pulsed packed	10.00
Torab-Mostaedi[13]	Hanson Mixer-Settler	7.08
Torab-Mostaedi[15]	pulsed disc and doughnut	7.32
This work	Kuhni column	5.70

## 8. CONCLUSIONS

In this work, an experimental study of mean drop size and flooding velocity in a Kühni extraction column was presented. The effects of agitation speed, dispersed phase and continuous phase flow rates, on drop sizes and flooding velocity were introduced. The results showed that Sauter-mean drop diameter is strongly affected by agitation speed as well as interfacial tension whereas volumetric flow rates of the dispersed and continuous phase have almost no significant effect. Sauter-mean drop diameter decreases with both increases in rotor speed and decrease in interfacial

tension. Two rigorous empirical correlations for predictions of flooding velocity and drop size diameter in Kühni columns were presented. The correlations are functions of operating variables, the physical properties of liquid systems and column geometry. The results showed that the maximum throughput decreases with the increase in agitation speed and flow ratio, while it increases with the increase in interfacial tension. The predictive correlations can be used for prediction of maximum capacity of existing Kühni columns and final sizing of the column diameter.

## 9. REFERENCES

- Ozawa, M., Suzuki, S. and Takeshita, K., "Advanced hydrometallurgical separation of actinides and rare metals in nuclear fuel cycle", *Solvent Extraction Research and Development, Japan*, Vol. 17, No. 0, (2010), 19-34.
- Habaki, H., Yoshimura, Y. and Egashira, R., "Liquid-liquid equilibrium extraction of aromatic compounds from model hydrocarbon mixtures for separation of cracked oils", *Solvent Extraction Research and Development, Japan*, Vol. 20, No. 0, (2013), 169-174.
- Habaki, H., Shimada, Y. and Egashira, R., "Separation of coal tar absorption oil by an ionic liquid supported liquid membrane", *Solvent Extraction Research and Development, Japan*, Vol. 20, No. 0, (2013), 175-181.
- Sadmezhad, S. and Alamdari, E.K., "Thermodynamics of extraction of  $zn^{2+}$  from sulfuric acid media with a mixture of dehpaa and mehpa", *International Journal Of Engineering Transactions B*, Vol. 17, (2004), 191-200.
- Hosseinzadeha, M., Alizadeh, M., Ranjbara, M. and Pazoukib, M., "Improvement of the solvent extraction of rhenium from molybdenite roasting dust leaching solution using counter-current extraction by a mixer-settler extractor", *International Journal of Engineering-Transactions A: Basics*, Vol. 27, No. 4, (2013), 651-658.
- Nabli, M.A., Guiraud, P. and Gourdon, C., "Cfd contribution to a design procedure for discs and doughnuts extraction columns", *Chemical Engineering Research and Design*, Vol. 76, No. 8, (1998), 951-960.
- Bastani, D., "Stagewise modeling of liquid-liquid extraction column (rdc)", *International Journal Of Engineering Transactions B*, Vol. 17, No. 1, (2004), 7-17.
- Nii, S., Suzuki, J., Tani, K. and Takahashi, K., "Mass transfer coefficients in mixer-settler extraction column", *Journal of chemical engineering of Japan*, Vol. 30, No. 6, (1997), 1083-1089.
- Pietzsch, W. and Pilhofer, T., "Calculation of the drop size in pulsed sieve-plate extraction columns", *Chemical engineering science*, Vol. 39, No. 6, (1984), 961-965.
- Yaparalvi, R., Das, P., Mukherjee, A. and Kumar, R., "Drop formation under pulsed conditions", *Chemical engineering science*, Vol. 41, No. 10, (1986), 2547-2553.
- Kumar, A. and Hartland, S., "Unified correlations for the prediction of drop size in liquid-liquid extraction columns", *Industrial & engineering chemistry research*, Vol. 35, No. 8, (1996), 2682-2695.
- Misek, T., Berger, R. and Schröter, J., "Standard test systems for liquid extraction studies", *EFCE Publ. Ser.*, Vol. 46, No. 1, (1985).
- TORAB, M.M., SAFDARI, J. and ASADOLLAHZADEH, M., "Mean drop size and drop size distribution in a hanson mixer-settler extraction column", (2012).
- Godfrey, J.C. and Slater, M.J., "Liquid-liquid extraction equipment, Wiley Chichester, UK, and New York, (1994).
- Torab-Mostaedi, M., Ghaemi, A. and Asadollahzadeh, M., "Flooding and drop size in a pulsed disc and doughnut extraction column", *Chemical Engineering Research and Design*, Vol. 89, No. 12, (2011), 2742-2751.
- Spaay, N., Simons, A. and Ten Brink, G., "Design and operation of a pulsed packed column for liquid-liquid extraction", in Proc. Internal. Solvent Extraction Conf., ISEC. Vol. 71, (1971), 19-23.
- Kumar, A. and Hartland, S., "Gravity settling in liquid/liquid dispersions", *The Canadian Journal of Chemical Engineering*, Vol. 63, No. 3, (1985), 368-376.
- Calabrese, R.V., Chang, T. and Dang, P., "Drop breakup in turbulent stirred-tank contactors. Part i: Effect of dispersed-phase viscosity", *AIChE Journal*, Vol. 32, No. 4, (1986), 657-666.
- Rinconrubio, L., Kumar, A. and Hartland, S., "Drop-size distribution and average drop size in a wirz extraction column", *Chemical engineering research & design*, Vol. 72, No. 4, (1994), 493-502.
- Kumar, A. and Hartland, S., "Correlations for prediction of mass transfer coefficients in single drop systems and liquid-liquid extraction columns", *Chemical Engineering Research and Design*, Vol. 77, No. 5, (1999), 372-384.
- Torab-Mostaedi, M., Safdari, J. and Torabi-Hokmabadi, F., "Prediction of mean drop size in pulsed packed extraction columns", *Iranian Journal of Chemical Engineering*, Vol. 8, No. 4, (2011).
- Ousmane, S., Isabelle, M., Mario, M.-S., Mamadou, T. and Jacques, A., "Study of mass transfer and determination of drop size distribution in a pulsed extraction column", *Chemical Engineering Research and Design*, Vol. 89, No. 1, (2011), 60-68.
- Asadollahzadeh, M., Torab-Mostaedi, M., Shahhosseini, S. and Ghaemi, A., "Experimental investigation of dispersed phase holdup and flooding characteristics in a multistage column extractor", *Chemical Engineering Research and Design*, Vol. 105, (2016), 177-187.
- Hemmati, A., Shirvani, M., Torab-Mostaedi, M. and Ghaemi, A., "Hold-up and flooding characteristics in a perforated rotating disc contactor (prdc)", *RSC Advances*, Vol. 5, No. 77, (2015), 63025-63033.
- Kennedy, J., Particle swarm optimization, in Encyclopedia of machine learning. 2011, Springer.760-766.
- Engelbrecht, A.P., "Fundamentals of computational swarm intelligence, John Wiley & Sons, (2006).
- Holland, J.H., "Adaptation in natural and artificial systems. An introductory analysis with application to biology, control, and artificial intelligence", *Ann Arbor, MI: University of Michigan Press*, (1975).
- Goldberg, D.E., "Genetic algorithms in search optimization and machine learning, Addison-wesley Reading Menlo Park, Vol. 412, (1989).
- Grefenstette, J.J. and Baker, J.E., "How genetic algorithms work: A critical look at implicit parallelism", in Proceedings of the third international conference on Genetic algorithms, Morgan Kaufmann Publishers Inc. (1989), 20-27.
- Samani, M.G., Asl, A.H., Safdari, J. and Torab-Mostaedi, M., "Drop size distribution and mean drop size in a pulsed packed extraction column", *Chemical Engineering Research and Design*, Vol. 90, No. 12, (2012), 2148-2154.



## Experimental Investigation of Flooding and Drop Size in a Kuhni Extraction Column

A.R. Shirvani,<sup>a</sup> A. Ghaemi<sup>a</sup>, M. Torab-Mostaedi<sup>b</sup>

<sup>a</sup> Department of Chemical Engineering, Iran University of Science and Technology

<sup>b</sup> Nuclear Fuel Cycle Research School, Nuclear Science and Technology Research Institute

---

### PAPER INFO

چکیده

---

#### Paper history:

Received 18 October 2015

Received in revised form 20 February 2016

Accepted 03 March 2016

---

#### Keywords:

Kuhni Column

Flood Point

Holdup

Sauter-Mean Drop Diameter

در این تحقیق، قطر متوسط ساتر و رفتار طغیان به صورت تجربی در یک ستون استخراج کوهنی مورد بررسی قرار گرفته است. آزمایشات تجربی بدون انجام انتقال جرم برای دو سیستم شیمیایی استاندارد انجام گرفته است. در آزمایشات پارامترهای عملیاتی شامل دور همزن، دبی هر دو فاز و کشش سطحی مطالعه شده است. قطر متوسط قطره، سرعت طغیان و ماندگی در حالت طغیان در ستون کوهنی اندازه گیری شده است. نتایج نشان داد که قطر متوسط ساتر به سرعت همزن و کشش سطحی وابسته بوده اما اثرات دبی فاز پیوسته و فاز پراکنده ناچیز می باشد. دو رابطه تجربی دقیق برای پیش بینی سرعت طغیان و اندازه متوسط قطره با متوسط انحراف به ترتیب  $0/7$  و  $7/2$  درصد ارائه گردید. رابطه متوسط قطر قطره تابعی از هندسه ستون، شرایط عملیاتی و خصوصیات سیستم های مایع می باشد. تطابق خوبی بین داده های تجربی و مقادیر پیش بینی شده توسط داده های روابط ارائه شده در کلیه شرایط عملیاتی برقرار می باشد.

**doi:** 10.5829/idosi.ije.2016.29.03c.02

---